MAPPING SNOW COVER ON MOUNT RAINIER, WA: SYNTHETIC APERTURE RADAR COMPARED TO MODIS VISUAL IMAGERY

Kate Baustian[1], Summer Rupper[2], Rick Forster[3], and McKenzie Skiles[4]

ABSTRACT

In order to constrain the effects of climate change in mountain watersheds, an understanding of the spatial extent and timing of snowmelt is necessary. However, lack of field records and difficultly modeling in remote and complex terrain, lead to uncertainty in precipitation and temperature measurements across many mountainous regions. In this study, Synthetic Aperture Radar (SAR) data from the European Space Agency's Sentinel-1 satellite is used to map wet snow over Water Year 2016 on Mount Rainier, a stratovolcano in the Cascade Range of Western Washington. Then, SAR wet snow maps are compared to a MODIS-derived factional snow-covered area product called MODSCAG. Results match an expected seasonal pattern while demonstrating the potential of SAR to provide high temporal and spatial resolution information that is not currently captured in common snow-covered area products. In the future, SAR could be used to improve understanding of snowpack characteristics in the Western United States. (KEYWORDS: Synthetic Aperture Radar, MODIS, MODSCAG, remote sensing, snow covered area, wet snow)

INTRODUCTION

Snowmelt is a critical part of the hydrologic cycle in many regions around the world (Barnett et al., 2008). In the US Intermountain West and California, over 60% of annual precipitation falls as snow, providing around 75% of annual stream discharge (Balk & Elder, 2000; Serreze et al., 1999). Humans use water from snowmelt for domestic consumption, agriculture and industry. Regional ecosystems are also dependent on the quantity, timing, temperature & mineral content of snow and glacier melt (Brown et al., 2007).

Changing patterns of human resource use, exacerbated by changes in climate, are shifting hydrologic cycles around the world (Vörösmarty et al., 2000). Studies have recorded declining snowpack along with earlier melt in the Western US (Barnett et al., 2008; Hamlet et al., 2005). In order to assist water and ecosystem managers in mitigating the effect of these changes, scientists are working to better understand snow cover and melt timing in alpine watersheds.

Unfortunately, precipitation is notoriously difficult to measure, especially when it is frozen and falling on complex terrain (Rasmussen et al., 2012). Currently, remote sensing is the only feasible tool for monitoring the spatial distribution of snow. Radar remote sensing is very appropriate for studying snowpack characteristics because radar waves can penetrate through clouds, do not require illumination of the Earth's surface by sunlight, and convey information about snowpack structure that is impossible to measure with visual imagery (Nolin, 2010). For example, wet and dry snow have dramatically different signatures in radar imagery. Synthetic Aperture Radar (SAR) is a type of active radar remote sensing that has excellent spatial resolution. With the recent launch of several new SAR satellites, now some SAR datasets also have excellent temporal resolution (ESA, 2017a).

In this study, data from the European Space Agency (ESA) Sentinel-1 SAR sensor is used to create wet snow distribution maps over Mount Rainier during Water Year 2016. SAR wet snow maps are then compared to the MODSCAG fractional snow-covered area product, which is created from Moderate Resolution Imaging Spectroradiometer (MODIS) visual imagery following a method developed by Painter et al. (2009). The two products are also combined to create multi-sensor wet snow probability maps.

Paper presented Western Snow Conference 2018

[1] Kate Baustian, University of Utah, Department of Geography, Salt Lake City, UT, kbaustian@gmail.com
[2] Summer Rupper, University of Utah, Department of Geography, Salt Lake City, UT, summer.rupper@geog.utah.edu
[3] Rick Forster, University of Utah, Department of Geography, Salt Lake City, UT, rick.forster@geog.utah.edu
[4] McKenzie Skiles, University of Utah, Department of Geography, Salt Lake City, UT, m.skiles@utah.edu

BACKGROUND

SAR sensors emit pulses of energy at a wavelength in the microwave part of the electromagnetic spectrum. After each pulse hits a target on Earth's surface, the amount of energy reflected back to the SAR antenna is measured. Radar backscatter values convey information about target material properties. Until recently, radar data was often difficult to access and process. Over the past three years, the ESA has facilitated free distribution of Sentinel-1 data at excellent temporal and spatial resolution along with development of well-documented, open-source, and relatively simple SAR processing programs (ESA, 2017a; ESA, 2017b). Now, SAR data is accessible to a variety of researchers and resource managers.

Microwaves easily pass through dry snow, but the presence of water in snow dramatically increases the dielectric constant which increases absorption and decreases backscatter. Wet snow is easy to detect with SAR because it has a much lower radar backscatter value than dry snow or snow-free ground. Austrian scientists Nagler and Rott developed a simple algorithm for mapping wet snow from SAR data based on backscatter changes between a reference image and an image containing wet snow. After extensive fieldwork in the Alps and Iceland, Nager and Rott determined that the reduction in backscatter amplitude from a snow free or dry snow pixel to a pixel covered by wet snow can be conservatively estimated at -3 decibels (Nagler & Rott, 2000). This method proved to be very effective at mapping snow and has been used by many other researchers (e.g. Malnes & Guneriussen, 2002; Rondeau-Genesse et al., 2016). Operational water resource management programs that use the Nagler and Rott (2000) method are currently being developed in Europe (Karna et al., 2002). However, no studies using SAR to map wet snow in the Western US have been published to date.

Inspired by Nagler and Rott's work, Malnes and Guneriussen (2002) designed an algorithm to create a wet snow probability map instead of a binary wet snow map. Their method also uses the difference between a wet snow image and a reference image, but in a second step Malnes and Guneriussen used a hyperbolic tangent function to assign backscatter difference values to a probability of wet snow between 0 and 100%. Additionally, Malnes and Guneriussen added parameters that calibrate data to an individual watershed. This algorithm was adapted by Rondeau-Genesse et al. (2016) to map snow cover in the Coast Mountains of British Columbia. Rondeau-Genesse et al., then combined SAR wet snow probability maps with MODIS snow covered area (SCA) products in an attempt to create improved wet snow-covered area maps with a multi-sensor approach.

MODIS provides nearly daily imagery of most of Earth's surface and NASA offers a daily SCA product derived from a Normalized Difference Snow Index (NDSI) algorithm applied to MODIS data (Hall et al., 2002). This information is invaluable to research and monitoring of changes in snow- and ice-covered area, but the high temporal resolution is balanced by a very low spatial resolution of 500 meters. Errors in the MODIS SCA product can arise from mixed land cover classes in the large pixels. To address this problem, Painter et al. (2009) developed an improved algorithm for mapping fractional snow-covered area from MODIS data using spectral unmixing. This method is used to produce an improved MODIS fractional SCA product called MODSCAG. Currently, MODSCAG is the best daily snow-covered area product available (Rittger et al., 2013).

The goal of this project is to assess the feasibility of using SAR combined with visual imagery to map wet snow in the Western US, following the algorithm used by Rondeau-Genesse et al. (2016) based on work by Nagler and Rott (2000) and Malnes and Guneriussen (2002). The Rondeau-Genesse et al. algorithm was chosen because their study area in Western British Columbia is similar to our study area in Western Washington state. However, instead of MODIS SCA, the MODSCAG product will be used as a validation dataset for SAR wet snow maps and to create wet snow probability maps through a multi-sensor approach. This may be the first study that uses SAR to map wet snow in the Western US and also the first study to combine SAR with the MODSCAG product.

STUDY AREA

In the US Pacific Northwest, approximately 50% of annual precipitation falls as snow (Serreze et al.,1999). Along with providing a critical source of domestic and industrial water, snowmelt is inextricably tied to local, lucrative salmon fishing and hydroelectric power industries (Kareiva et al., 2000). Incidentally, some of the earliest American studies of snow and ice contribution to streamflow occurred in this region (Fountain & Tangborn,1985; Tangborn & Rasmussen, 1976).

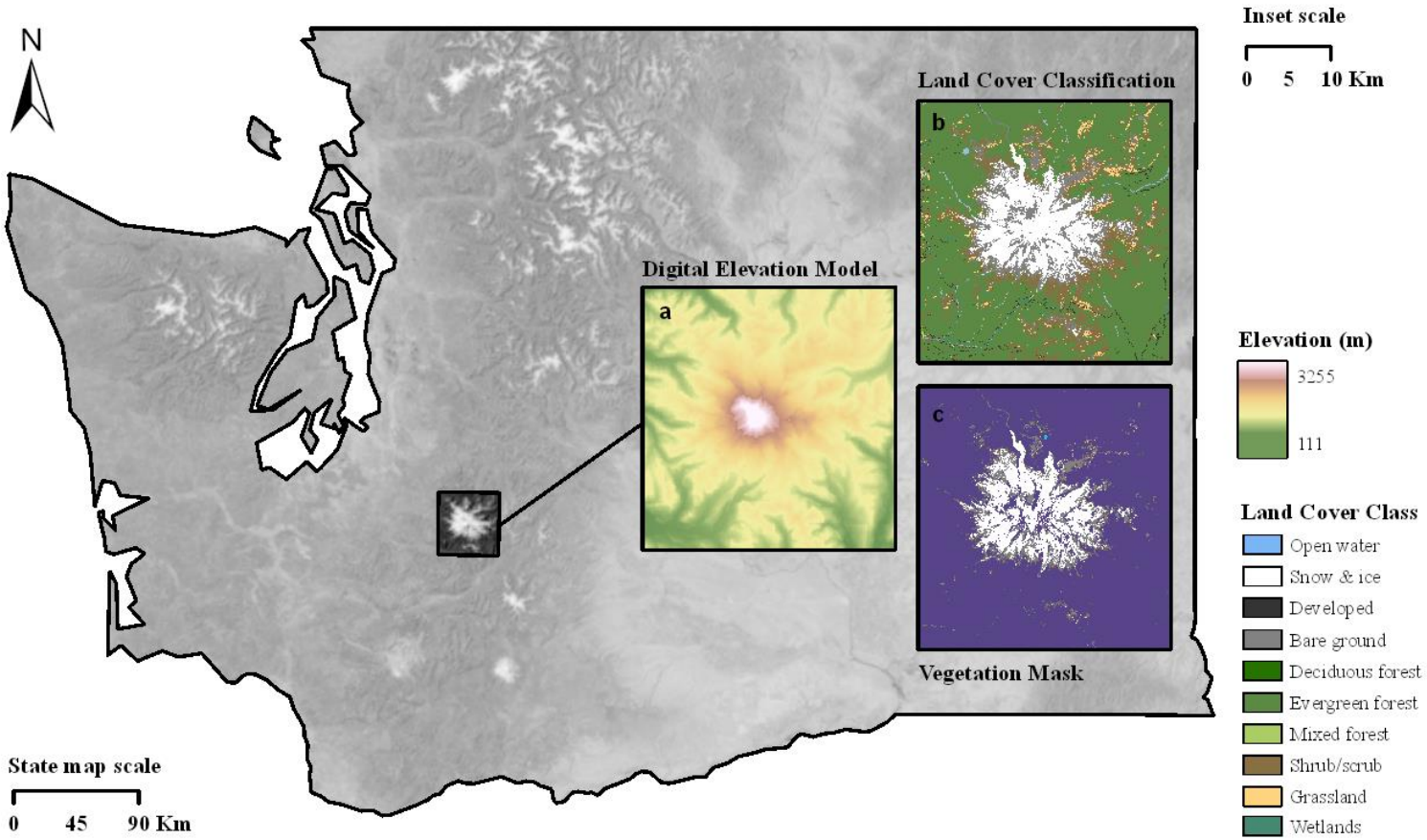

Figure 1: Location of study area around Mount Rainier, a stratovolcano in the Cascade Range of Western Washington. Study area is 30 Km by 30 Km. Topography and land cover type are shown in Insets (**a**) and (**b**), respectively. In this study pixels of all land cover classes are used. However, in many SAR studies vegetated pixels are masked. Inset (**c**) shows a mask of vegetated pixels to demonstrate the significant loss of information when vegetated pixels are masked.

Grayscale basemap courtesy of ESRI ArcGIS Map Service
Shuttle Radar Topography Mission 1 Arc-second Digital Elevation Model Version 3 courtesy of NASA Jet Propulsion Laboratory (2013)
Land Cover Classification data courtesy of US Multi-Resolution Land Characteristics Consortium (2015)

Mount Rainier provided an effective natural laboratory for this study because it is covered by extensive snow above tree line, which minimizes seasonal changes in radar reflectance due to vegetation. A study area of 30 kilometers by 30 kilometers was chosen with a maximum elevation of 4,393 meters in elevation and centered at 46.85˚ N.

DATA

Sentinel-1 is a constellation of two identical C-band SAR satellites, traveling in near polar, sun synchronous, opposite and complementary orbits with a nominal spatial resolution of approximately 10 meters. Sentinel-1A was launched in April of 2014 and Sentinel-1B was launched in April of 2016 (ASF, 2017). Since Sentinel-1B was not fully operational for the duration of this study, all SAR images used in this study were acquired by Sentinel-1A. Pre-processed radar data products were acquired from the Alaska Satellite Facility's Vertex website (ASF DAAC, 2015-2016). Although datasets are available at various levels of processing, only Ground Range Detected (GRD) data was used. GRD products have been resampled to account for different pixel size in the azimuth and range directions and projected onto an ellipse. In this study, the SAR data was further resampled to a 30-meter spatial resolution to match the SRTM 1-Arc second DEM, which was used during several processing steps (Figure 2). In order to account for changes due to slight variations in satellite geometry, data was also limited to one exact repeat path and polarization: VV-polarized, descending Path 115. This combination of path and polarization was chosen because it provided the maximum quantity of data covering the study region and time frame. SAR imagery from Path 115 was acquired between 6:20 and 7:20 AM Pacific Standard Time.

MODSCAG fractional snow-covered area data was acquired courtesy of the NASA Jet Propulsion Laboratory. Images were downloaded for dates corresponding to acquisition of SAR images, along with six days prior. Since cloud cover has been flagged in MODCAG products, a simple temporal filter was designed to prioritizing snow pixel values in the most recent MODCAG image. Unfortunately, issues with high cloud identification in the MODSCAG product limited the applicability of this filter. Therefore, the best cloud-free MODSCAG image was chosen manually from a seven-day window before and including the date of SAR scene acquisition (Figure 2, Box III). Excellent cloud free images were often available during the late spring and summer melt season. In contrast, many winter images obscured by clouds over the entire window (Figure 3).

METHODS

Processing of GRD SAR data was completed using the SNAP Sentinel-1 Toolbox, an open-source program for working with SAR data developed by the ESA (ESA, 2017b). Basic Sentinel-1 processing steps are shown in Figure 2, Section I. First, a precise orbit file was applied to each image. Next, rasters were subset to reduce processing time and a filter was applied to remove known thermal noise. Images were calibrated to $Beta_0$, which converts the sensor data into radar backscatter values. All the images were co-registered using pixel location and a DEM. Then, a multi-temporal speckle filter was applied to stacks of images grouped by season and the DEM was again used to remove changes in backscatter due to topography (Small, 2011).

Figure 2, Box II shows the workflow for detecting wet snow using radar backscatter changes from a reference image, following Nager and Rott (2002). Since it is impossible to find a SAR scene with no snow or all dry snow in our study area, a reference image was created by averaging six scenes with the smallest area and most diverse pattern of wet snow cover. Then, ratios of each SAR image to the reference were computed.

Backscatter ratio values were converted to wet snow probability using the following equation:

$$F(x) = 50 - 50\tanh[a(x+3)]\,\%$$

This equation was developed by Malnes and Guneriussen (2002) and used by Rondeau-Genesse et al. (2016). The ratio between a SAR wet snow scene and the reference image equals *x*. A 50% probability of wet snow is designated as -3 decibels, which is the ratio value recommended by Nagler and Rott (2002) to represent wet snow. Hyperbolic tangent directs ratio values to a new value between -1 and 1. Positive values indicate a smaller change of backscatter than the -3 decibel threshold. Negative values indicate a larger change of backscatter than the -3 decibel threshold. Wet snow probability values below or above 50% are assigned, respectively.

Parameter *a* is used to adjust for elevation changes across the image. In this study, an *a* of 0.75 was chosen, following Rondeau-Genesse et al. (2016).

After pixels were assigned a probability of being wet snow using the SAR reference-ratio method, they were filtered based on elevation and proximity to pixels with snow according to the MODSCAG product. Following Rondeau-Genesse et al. (2016), pixels designated as wet snow by SAR but lower than 1500 meters and further than 1.5 kilometers from a MODSCAG snow pixel were re-assigned a very low probability of being wet snow. In our high elevation study area, very few SAR wet snow pixels were eligible to be removed by the low elevation mask.

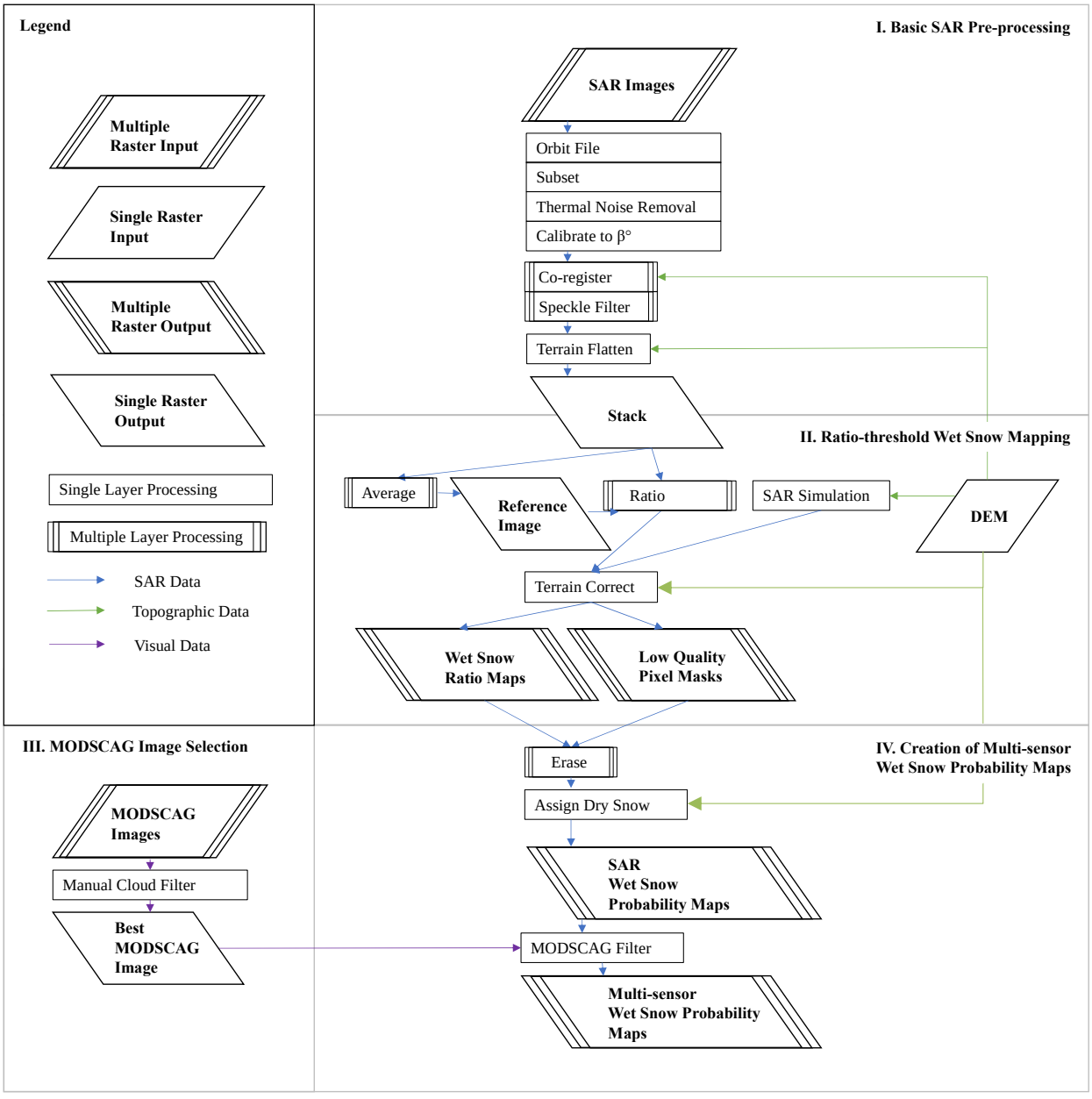

Figure 2. Workflow of processing steps for SAR and MODSCAG imagery.

After wet snow probability maps were created with SAR and filtered with MODSCAG, a few more masks were applied. First, high elevation zones with a low probability of wet snow were marked as regions that may contain dry snow. These pixels were marked to aid in interpretation of wet snow maps because dry snow is invisible in SAR imagery but important for water resource management. Once again following the algorithm of Rondeau-Genesse et al. (2016), areas higher than the mean elevation of wet snow, plus one standard deviation times a recommended calibration factor of 1.6, were marked as dry snow. Finally, pixels flagged for quality issues were erased, including those with DEM gaps, extreme SAR incidence angles, or radar layover and shadow.

RESULTS AND DISCUSSION

Seven-day cloud-filtered MODSCAG images are shown in Figure 3. Notably, MODSCAG imagery appears to have adequate resolution to be used as validation for, or in combination with, SAR data at spatial scales on the order of our Mount Rainier study area. Results show that heavy clouds consistently block visual imagery during the winter in this region. Clouds limit the use of MODSAG products as validation for SAR wet snow maps, however, they also suggest that SAR snow maps could provide useful information to scientists when visual data is blocked for a significant portion of the year.

Some issues with high cloud recognition in the MODSCAG product, which inhibited use of an automatic cloud filter, are also apparent in Figure 3. For example, on October 8th grayscale values are indicating various fractions of snow cover across the entire study area. Considering the season, these pixels are likely high clouds that resemble snow in the visual imagery.

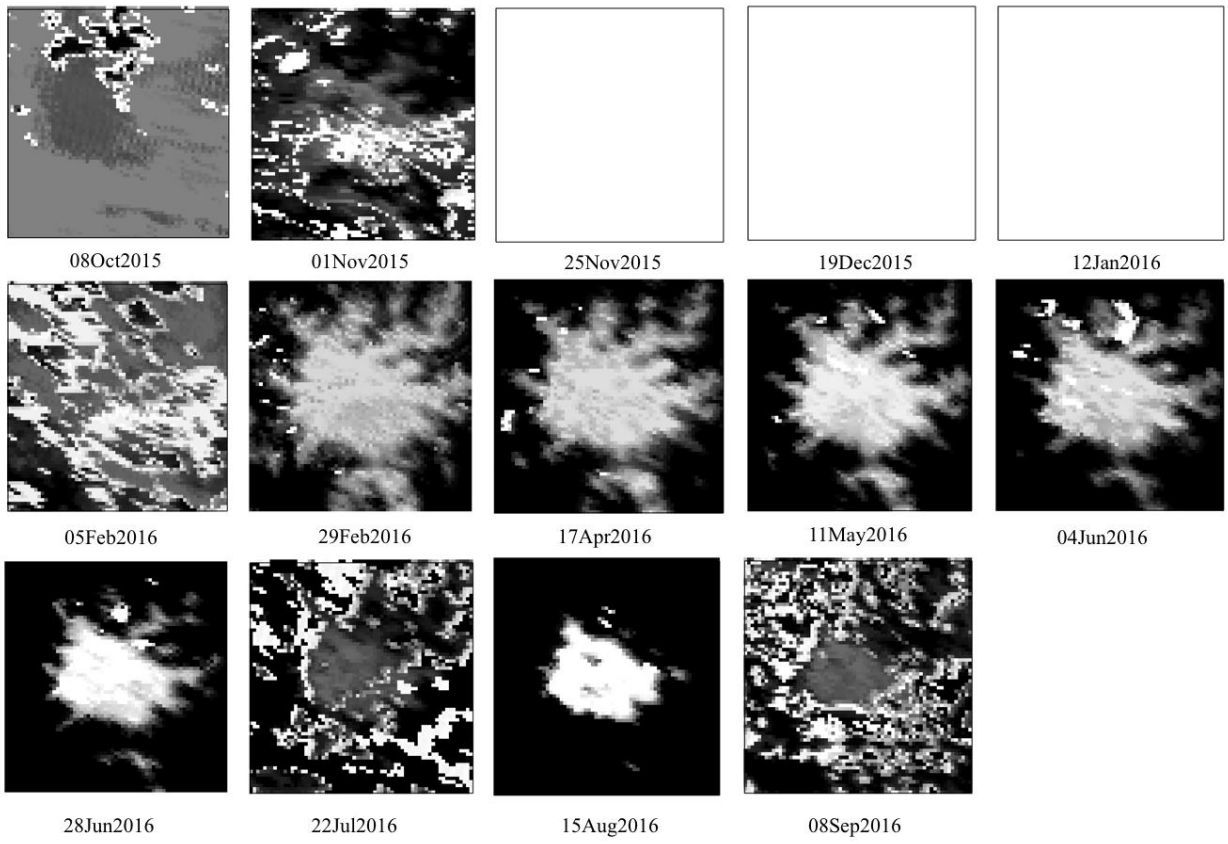

Figure 3. MODCAG images used in this study courtesy of the NASA Jet Propulsion Laboratory and created with the algorithm developed by Painter et al. (2009). These images were manually chosen to have minimum cloud cover from a seven-day window ending on the date of SAR data acquisition. Black to gray values show fractional snow cover with lighter colors corresponding to greater fractional cover. True white values signify cloud cover.

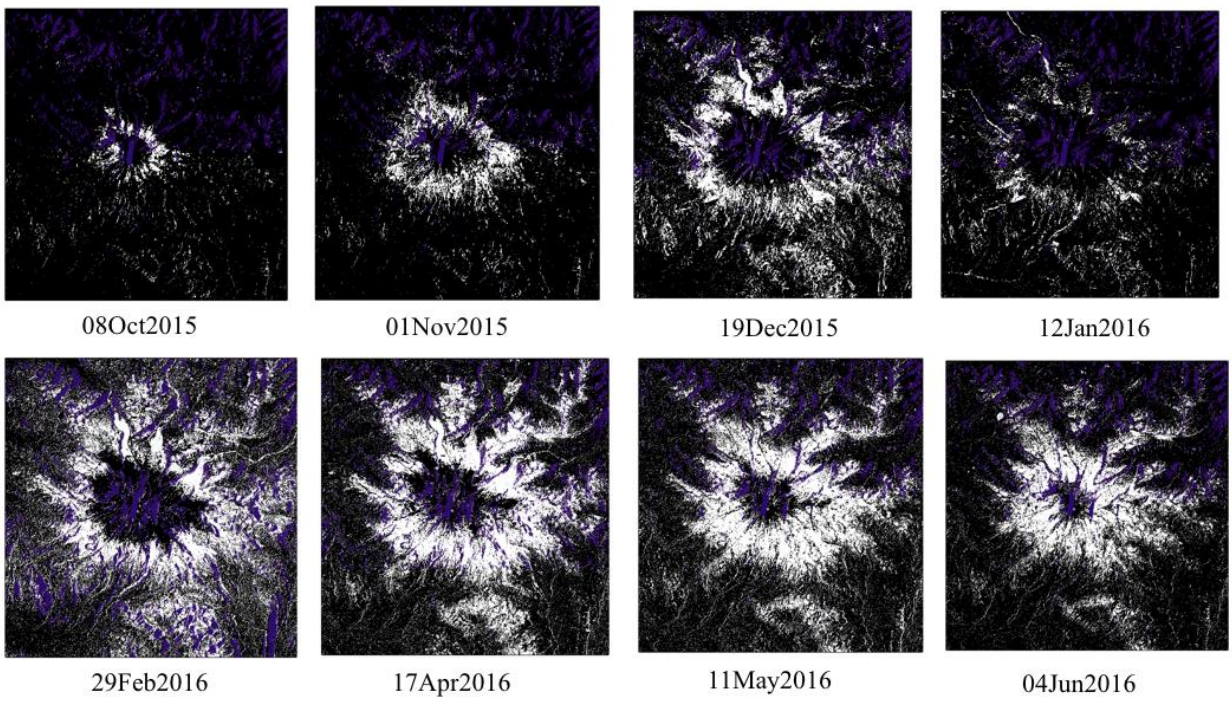

(a)

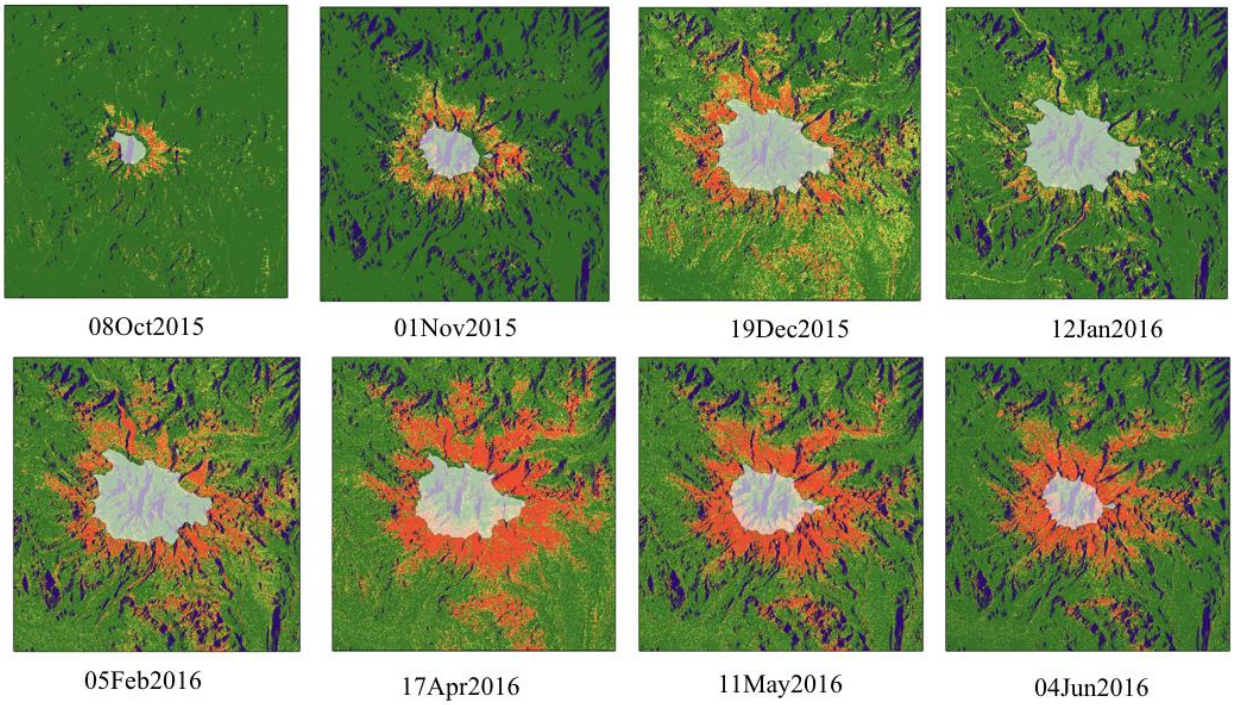

(b)

Figure 4 (a): Selected SAR binary wet snow maps created with a stationary threshold of -3 decibels. Pixels designated as wet snow are white. Pixels designated as either dry snow or no snow are black. Pixels with questionable data are masked in purple. (b): Sample wet snow probability maps created by combining SAR and MODSCAG data following Rondeau-Genesse et al. (2016). Pixels with a high probability of being wet snow are warm colors. Pixels with a low probability of being wet snow are cooler colors. Transparent white polygons delineate areas that are likely dry snow.

Binary SAR wet snow maps created the reference-ratio method are shown in the upper panel of Figure 4. An expected seasonal pattern of wet snow-covered area is visible. In late fall, snow cover is at a minimum. During this time, snow is only present at the highest elevations and all snow-covered area is wet. In early winter, dry snow likely covers much of the study area and wet snow-covered area is at a minimum. In late winter, snow cover extends to lower elevations where a ring of wet snow develops around the volcano. The ring of wet snow expands until April, then retreats through the melt season until the minimum extent of snow returns again in late fall.

Wet snow probability maps are shown in the lower panel of Figure 4. In general, they appear quite similar to binary wet snow maps created with a stationary threshold (shown in the upper panel of Figure 4). This is because pixels marked as wet snow in the binary maps are strongly mapped to 100% probability of wet snow. A qualitative comparison of maps in both panels of Figure 4 suggests that wet snow probability maps do not contain much more information than binary wet snow maps created with a stationary threshold. Therefore, the algorithm developed by Malnes and Guneriussen (2002) and used by Rondeau-Genesse et al. (2016), is likely not more accurate than the method developed by Nagler and Rott (2000).

In SAR studies of wet snow, it is common to mask pixels covered by heavy vegetation because vegetation can have large seasonal changes in radar backscatter that resemble seasonal changes from snow cover. In this study vegetated pixels were not removed, although dense vegetation is present at low elevations (Figure 1). Pixels were not masked in order to assess whether a multi-sensor approach was able to improve the quality of data in zones with high SAR uncertainty. Results show that the MODSCAG filter did remove noise from the SAR wet snow scenes although this effect would be greater for a larger study area due to the spatial resolution of MODIS imagery.

Dry snow-covered area estimated from SAR data is shown on wet snow probability maps in the lower panel of Figure 4. Since SAR imagery cannot identify dry snow, dry snow-covered pixels were assigned based on spatial distribution of wet snow and elevation data. Dry snow polygons roughly match fractional snow-covered area in the MODSCAG imagery and areas without wet snow in the SAR probability maps. However, a constant elevation contour is used to assign dry snow. Therefore, some information about the spatial distribution of wet snow is lost. For example, on April 17th wet snow is present at higher elevations on south facing slopes than on north facing slopes. This aspect signal is smoothed in the dry snow-covered area polygon. Future studies should use visual imagery to map dry snow-covered area in order to capture true spatial variation in the distribution of wet snow and avoid over-estimating wet snow-covered area in high elevation zones that are snow-free.

CONCLUSIONS

In conclusion, Sentinel-1 data can provide unique and important information about seasonal snow and ice. A simple method comparing SAR wet snow scenes to a reference image can be used to map wet snow-covered area at high temporal and spatial resolutions, even without sunlight and below heavy cloud cover. Binary wet snow maps created with a stationary threshold of backscatter change provide approximately the same amount of information as maps of wet snow probability that consider a wider variation of backscatter changes. These methods were developed in Europe and have been used extensively around the world. However, this study was the first application in the Western US and the first study that combined SAR imagery with the MODCAG fractional snow-covered area product. Results show that SAR can effectively be used to map wet snow distribution around Mount Rainier and multi-sensor approaches combining SAR with visual imagery have great potential to assist scientists and water resource managers across the western US.

REFERENCES

ASF (2017). Sentinel-1. Retrieved from https://www.asf.alaska.edu/sentinel/data/.

ASF DAAC. 2015-2016. [Processed Sentinel-1 Data]. Contains modified Copernicus Sentinel data 2015. Retrieved from https://vertex.daac.asf.alaska.edu/, 2 April 2017.

Balk, B., & K. Elder. 2000. Combining binary decision tree and geostatistical methods to estimate snow distribution in a mountain watershed. *Water Resources Research*, *36*(1), 13-26.

Barnett, T. P., Pierce, D. W., Hidalgo, H. G., Bonfils, C., Santer, B. D., Das, T., ... & D. R. Cayan. 2008. Human-induced changes in the hydrology of the western United States. *science*, *319*(5866), 1080-1083.

Brown, L. E., Hannah, D. M., & A.M. Milner. 2007. Vulnerability of alpine stream biodiversity to shrinking glaciers and snowpacks. Global Change Biology, 13(5), 958-966.

ESA. 2017a. Sentinel-1 satellites observe snow melting processes. Retrieved from https://sentinels.copernicus.eu/web/sentinel/news/-/article/sentinel-1-satellites-observe-snow-melting-processes.

ESA. 2017b. SNAP - Sentinel Application Platform v6.0. Retrieved from http://step.esa.int.

Fountain, A. G., & W. V. Tangborn. 1985. The effect of glaciers on streamflow variations. Water Resources Research, 21(4), 579-586.

Hall, D. K., Riggs, G. A., Salomonson, V. V., DiGirolamo, N. E., & K. J. Bayr. 2002. MODIS snow-cover products. Remote sensing of Environment, 83(1-2), 181-194.

Hamlet, A. F., Mote, P. W., Clark, M. P., & D. P. Lettenmaier. 2005. Effects of temperature and precipitation variability on snowpack trends in the western United States. Journal of Climate, 18(21), 4545-4561.

Karna, J. P., Pulliainen, J., Huttunen, M., & J. Koskinen. 2002. Assimilation of SAR data to operational hydrological runoff and snow melt forecasting model. In Geoscience and Remote Sensing Symposium, 2002. IGARSS'02. 2002 IEEE International (Vol. 2, pp. 1146-1148). IEEE.

Kareiva, P., Marvier, M., & M. McClure. 2000. Recovery and management options for spring/summer chinook salmon in the Columbia River Basin. Science, 290(5493), 977-979.

Malnes, E., & T. Guneriussen. 2002. Mapping of snow covered area with Radarsat in Norway. In Geoscience and Remote Sensing Symposium, 2002. IGARSS'02. 2002 IEEE International (Vol. 1, pp. 683-685). IEEE.

Nagler, T., & H. Rott. 2000. Retrieval of wet snow by means of multitemporal SAR data. IEEE Transactions on Geoscience and Remote Sensing, 38(2), 754-765.

Nagler, T., Rott, H., Malcher, P., & F. Müller. 2008. Assimilation of meteorological and remote sensing data for snowmelt runoff forecasting. *Remote sensing of environment*, *112*(4), 1408-1420.

Nagler, T., Rott, H., Ripper, E., Bippus, G., & M. Hetzenecker. 2016. Advancements for snowmelt monitoring by means of Sentinel-1 SAR. *Remote Sensing*, *8*(4), 348.

NASA Jet Propulsion Laboratory. 2013. NASA Shuttle Radar Topography Mission United States 1 arc second. Version 3. 6oS, 69oW. NASA EOSDIS Land Processes DAAC, USGS EROS Center, Sioux Falls, South Dakota (https://lpdaac.usgs.gov), accessed Jan 17, 2018 http://dx.doi.org/10.5067/MEaSUREs/SRTM/SRTMUS1.003.

Nolin, A. W. 2010. Recent advances in remote sensing of seasonal snow. Journal of Glaciology, 56(200), 1141-1150.

Painter, T. H., Rittger, K., McKenzie, C., Slaughter, P., Davis, R. E. & J. Dozier. 2009. Retrieval of subpixel snow covered area, grain size, and albedo from MODIS. Remote Sensing of Environment 113(4), 868–879. doi:10.1016/j.rse.2009.01.001. Data accessed online on 2018-04-13 at snow.jpl.nasa.gov.

Rasmussen, R., Baker, B., Kochendorfer, J., Meyers, T., Landolt, S., Fischer, A. P., ... & C. Smith. 2012. How well are we measuring snow: The NOAA/FAA/NCAR winter precipitation test bed. *Bulletin of the American Meteorological Society*, *93*(6), 811-829.

Rittger, K., Painter, T. H., & J. Dozier. 2013. Assessment of methods for mapping snow cover from MODIS. Advances in Water Resources, 51, 367-380.

Rondeau-Genesse, G., Trudel, M., & R. Leconte. 2016. Monitoring snow wetness in an Alpine Basin using combined C-band SAR and MODIS data. *Remote Sensing of Environment, 183,* 304-317.

Serreze, M. C., Clark, M. P., Armstrong, R. L., McGinnis, D. A., & R. S. Pulwarty. 1999. Characteristics of the western United States snowpack from snowpack telemetry (SNOTEL) data. *Water Resources Research*, *35*(7), 2145-2160.

Small, D. 2011. Flattening gamma: Radiometric terrain correction for SAR imagery. *IEEE Transactions on Geoscience and Remote Sensing*, *49*(8), 3081-3093.

Tangborn, W. V., & L. A. Rasmussen. 1976. Hydrology of the North Cascades Region, Washington: 2. A proposed hydrometeorological streamflow prediction method. Water Resources Research, 12(2), 203-216.

Vörösmarty, C. J., Green, P., Salisbury, J., & R. B. Lammers. 2000. Global water resources: vulnerability from climate change and population growth. science, 289(5477), 284-288.